



journal homepage: www.brodogradnja.fsb.hr

Brodogradnja

An International Journal of Naval Architecture and Ocean Engineering for Research and Development



Small Modular AUV Based on 3D Printing Technology: Design, Implementation and Experimental Validation



Lichun Yang, Xianbo Xiang, Dian Kong, Shaolong Yang*

School of Naval Architecture and Ocean Engineering, Huazhong University of Science and Technology, 430074, Wuhan, China

ARTICLE INFO

Editor-in-Chief: Prof. Nastia Degiuli

Associate Editor: PhD Ivana Martić

Keywords:

Small Autonomous Underwater Vehicle (AUV)

Modularization

Autonomous control

3D Printing

Depth Tracking

ABSTRACT

A small modular autonomous underwater vehicle (AUV) offers several benefits including enhanced mobility, cost-effectiveness, compact and portable structure, and small size. This paper proposes a comprehensive design and implementation approach for a small modular AUV, named as ARMs1.0, utilizing cutting-edge 3D printing technology. The main cabin shell of the AUV features a modular design and is manufactured using 3D printing technology. The control module and sensing equipment are installed in a sealed compartment. To achieve forward, pitching, and yawing motions, the AUV is equipped with ducted propeller and four independent rudders. The modular approach in AUV design has been implemented, considering both the main cabin shell as well as the subsections and segments of the AUV. Additionally, a centralized control system architecture design is developed based on the specific tasks of the AUV. The composition and functions of key units are described in detail, and an autonomous depth-tracking control strategy is formulated. Based on the experimental results for AUV motion in horizontal and vertical planes, including autonomous depth tracking tests, the ARMs1.0 AUV demonstrates the capability to successfully perform required maneuvering tasks. The designed small modular AUV has achieved accurate depth tracking, precise heading following and exhibits excellent maneuverability.

1. Introduction

The autonomous underwater vehicles (AUVs) are widely being deployed to perform various research and scientific underwater exploration tasks in harsh and unpredictable ocean environment. The advantages of autonomous underwater vehicles (AUVs) include excellent environmental adaptability, a wide range of commercial and defence applications, ease of use, and various others [1,2]. The AUV is considered one of the most important and indispensable gadget in the domain of Ocean Engineering for efficient underwater exploration, data collection, and analysis. AUVs excel in diverse aquatic environments, perform various tasks autonomously, and operate with minimal human intervention. Their impact is significant, contributing to climate research, resource exploration, marine conservation, and improving the safety and efficiency of underwater operations. AUVs hold tremendous potential for further advancements in marine research and industry. The modern AUV design endeavours encompass AI-based autonomy, adaptive control strategies,

* Corresponding author.

E-mail address: xbxiang@hust.edu.cn

equipped with high-tech sensors and hydrodynamically efficient shapes and sizes [3]. The fixed configurations of AUVs pose challenge to meet the complex operational requirements and research pursuits. However, their modular design allows for easy upgrades, replacements, technical modernization, and reusability of functional components. Accordingly, modular designs of small size AUVs are considered more cost-effective and easier to build and market compared to large size AUVs, both in terms of utilization and cost [4,5].

This article presents the design and development of a small modular AUV named as ARMs1.0. The ARMs1.0 AUV has been designed and developed by the Lab of Advanced Robotic Marine Systems (ARMs), School of Naval Architecture and Ocean Engineering (SNAOE) at Huazhong University of Science and Technology (HUST) in Wuhan, China., for various applications which includes but not limited to:

1. Simulation verification Purposes: ARMs1.0 serves as a small self-developed model for which the maneuverability is tested and verified through underwater experiments. The experimental data subsequently also utilized as a basis for Computational Fluid Dynamics (CFD) simulations/analyses [6-8].

2. Algorithm Validation Purpose: ARMs1.0 acts as a reliable test platform for the development and evaluation of underwater path planning and tracking control algorithms, specifically for underactuated underwater vehicles.

3. Educational Purposes: ARMs1.0 is utilized for educational purposes. It plays a vital role in the Lab of ARMs, SNAOE at HUST. Primarily, ARMs1.0 provides a strong foundation for students to independently design and develop AUVs. It serves as a valuable educational tool, allowing students to gain practical experience in building and operating AUVs. Through hands-on involvement with ARMs1.0, students foster a deeper understanding of the field of underwater robotics.

The ARMs1.0 AUV is a compact torpedo-shaped autonomous underwater vehicle with a length of less than 1.5 meters, a diameter of 0.14 meters, and a dry mass of less than 10 kilograms. Its smaller size makes it easy to handle and user-friendly for assembly and conducting experiments [9-11]. The AUV's main features, considering its modularity, are as follows:

Precise Motion Control: The AUV achieves surge motion by means of controlling the stern ducted propeller. Steering, pitching, and other actions are performed by controlling the rudders. This allows for precise maneuverability in various underwater environments.

Cost-Effectiveness and Rapid Development: The AUV is designed to be low-cost, enabling rapid manufacturing and processing. Due to its shortened development cycle, the AUV is considered an efficient and practical choice for research and experimentation.

Modular Design and Scalability: The AUV is oriented towards modular design, providing strong scalability. It can easily change its appearance and adapt to specific requirements by incorporating different sensors and components.

Submarine Ballast Water System Simulation: The AUV simulates a submarine ballast water system, enabling it to achieve underwater static heave function. This feature improves the AUV's concealment and enhances its ability to operate stealthily.

By incorporating these above said features, the ARMs1.0 AUV offers a versatile, adaptable and modular platform for various underwater applications. The ARMs1.0 is smaller in size, lighter in weight, more portable and flexible, and have lower costs. Its compact size, modularity, and simulated ballast water system contribute to its maneuverability, scalability, and concealment capabilities, while maintaining a cost-effective and efficient design.

1. Mechanical structure design

Precisely, the AUV shown in Fig. 1 is 1.07 m long, having diameter 0.14 m, dry weight is 7.7 kg and AUV displacement volume is 8.26 L.

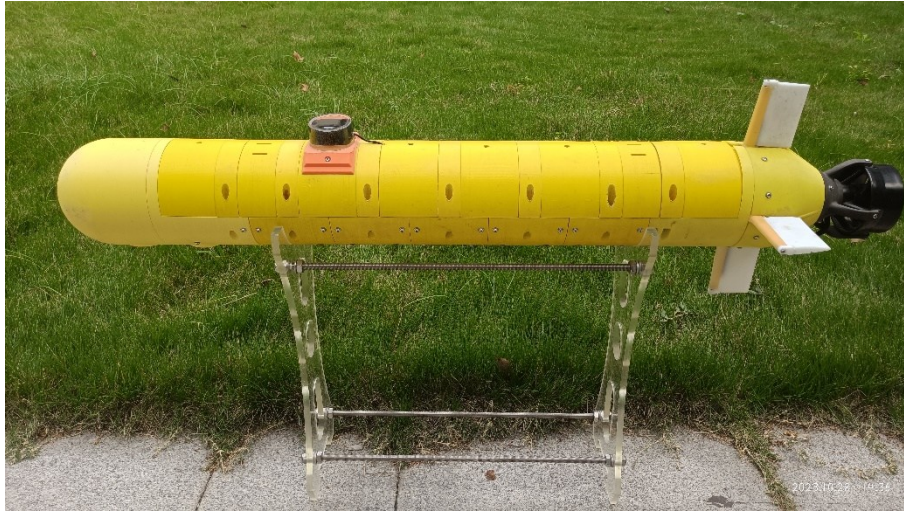


Fig. 1 AUV named as ARM1.0

1.1 Modular AUV design and architecture

The 3D CAD model of the AUV is shown in Fig. 2. The underactuated AUV features a torpedo-like shape, enabling it to generate forward propulsion through the water by means of a watertight stern shrouded propeller. The AUV is equipped with two vertical and two horizontal rudders, which are employed to control the rotation angles in both horizontal and vertical planes. The AUV's heading is controlled by the vertical rudders, while the horizontal rudders allow to achieve the maneuvering capability in vertical plane for ascending and descending operations of AUV.

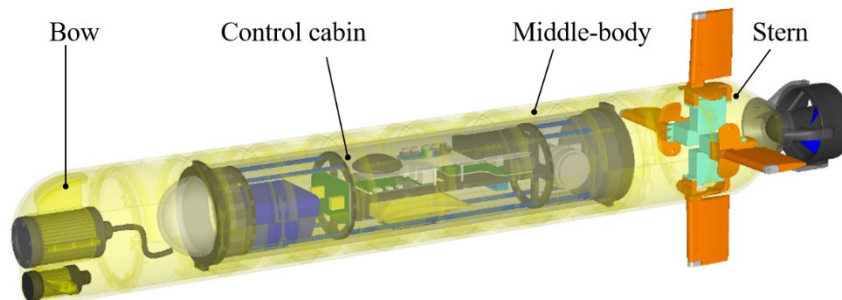


Fig. 2 Cabin display of ARM1.0

The AUV is mainly composed of four sections: bow section, middle-body section, stern section, and the internally placed watertight control cabin. These sections of the AUV hull-body are manufactured through 3D printing technology using an environmental friendly degradable plastic material known as PLA (Polylactic Acid). The control cabin, watertight steering gear, stern propeller, camera, LED, and other equipment are securely attached to the hull and the cabin of the underwater vehicle. This compact size modular design of AUV also provides flexibility to easily assemble and disassemble the sections of AUV for transportation purposes. The main parameters of AUV are given in the following Table 1.

Table 1 Main Parameters of AUV

Length (mm)	Diameter (mm)	Length-to-diameter ratio	Weight (kg)	Volume (L)	Max-Speed (kn)	Endurance (h)
1070	140	7.64	7.7	8.26	5.4	4

The modular design concept of ARM1.0 primarily focuses on the interconnection between the cabins and the segments/subsections of the middle-body section. The main advantages of the AUV's modular design are elaborated as under:

- **Easy to assemble and disassemble.** The modular design of ARMs1.0 enables swift assembling or disassembling of parts located outside the sealed cabin for maintenance purpose and/or equipment additions. Since, the sections and subsections are bolted together and the 3D printed casing does not require water tightness considerations, therefore, assembling/disassembling can be easily carried out. Additionally, 3D printing technology can be leveraged to design installation methods that align with the appearance of different devices, simplifying their installation and operation.

- **Expandability:** The modular design ensures a high level of adaptability in terms of both the AUV's physical structure and functionality. The addition or removal of segments enables the customization of the AUV's appearance to suit expanding or contracting requirements. For instance, to incorporate underwater hovering capabilities, segments with equipment such as Doppler Velocity Log (DVL), sonar, lateral and vertical thrusters can be added. The length of the sealed cabin can be modified, and segments on the middle-body section shell can be raised or reduced accordingly.

- **Practical for upkeep and iteration:** Maintenance and repair become more practical with a modular design. In case of a broken part, only the damaged portion needs to be dismantled, simplifying system maintenance and allowing for rapid prototyping. The time required to create new parts is significantly reduced. Modularization also facilitates quick product iteration, as only the updated portions need to be reprinted once the optimization design is complete.

1.2 Assembly of the sections and sub-sections

The sections and sub-sections of the AUV are connected using screws, which facilitate easy and quick disassembly of the components. In addition to the four essential compartments mentioned earlier, additional compartments like side or vertical thrusters shown in Fig. 3 and small sealed compartments for carrying other equipment can be inserted between the existing compartments, if required. This modular design allows for flexibility in incorporating additional functionalities or accommodating specific equipment needs.

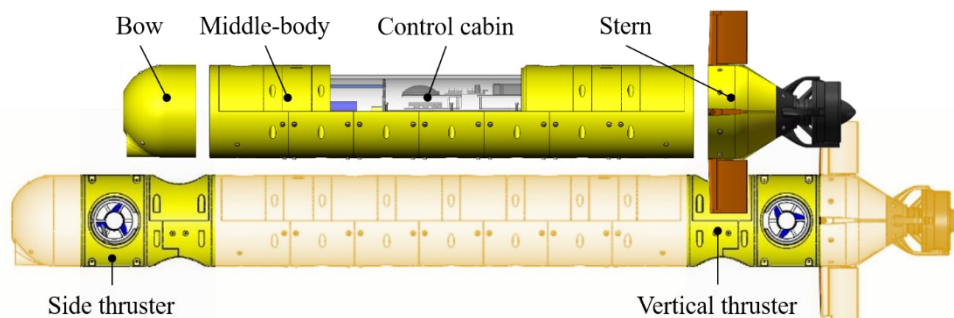


Fig. 3 Auxiliary thruster configuration of ARMs1.0

1.3 Modular rudder configuration

In the stern section, a conversion rudder structure is implemented, transitioning from a "cross" to an "X" rudder configuration. Fig. 4 illustrates the stern compartment, which incorporates four rudders symmetrically arranged and individually controllable. The middle-body section contains eight screw holes that correspond to the four holes present in the stern shell. When a change in rudder shape is required, the stern is rotated by 45° , and the control program is adjusted accordingly to accommodate the new rudder configuration. This design enables the comparison of different rudder shapes and facilitates the validation of algorithms specific to each rudder configuration.

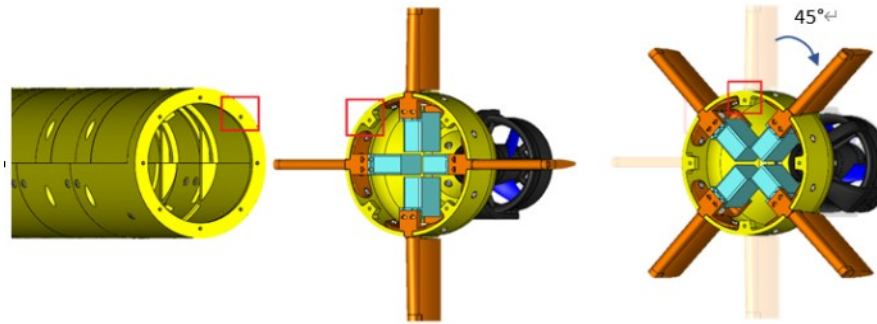


Fig. 4 Stern rudder shape conversion

1.4 The modular design of fragments

To speed up production, improve the overall robustness of the compartment, and save maintenance costs, the longest shell of the midship compartment is broken into various segments and printed in many portions, as illustrated in Fig. 5. Additionally, only the stressed segments in the lower half have screw holes design and the remaining surrounding segments are mechanically pushed and fixed resulting in minimizing the usage of screws and enable disassembly.

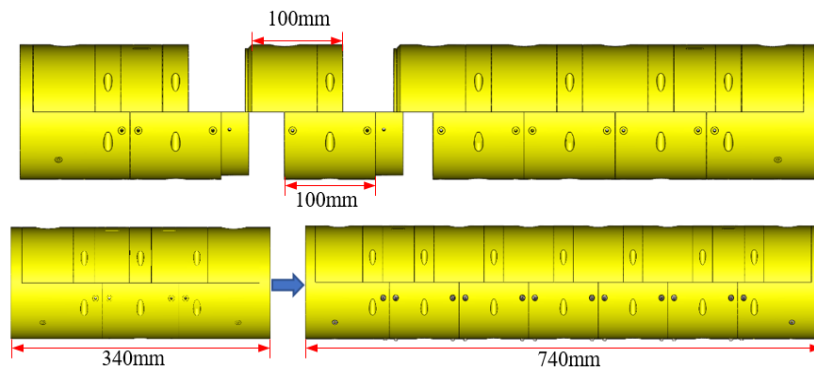


Fig. 5 Fragment modularization

The combined length of the upper two segments of the Middle-body section is equal to that of the lower segment, as shown in Fig. 5. Considering the four segments as one unit, the length of the segment can be altered to meet various size requirements by varying the number of groups the segment forms. The minimum length of the middle-body section is 340 mm, and each time the size modification is 100 mm.

The modular architecture of the AUV allows for the expansion or reduction of segments as required, making the printing process more manageable. The size limitations of common printers can make it difficult to adhere to the specifications of larger cabin components. Printing large components can lead to issues such as deformation and dislocation, which can increase the error rate. To mitigate these challenges, the modular design approach is employed, utilizing several smaller pieces to replace a single large part. This not only reduces the risk of errors but also enables faster printing times. Simultaneous use of multiple printers can further expedite the printing process.

2. Hardware and software system design

2.1 Hardware system architecture

The hardware system of the AUV consists primarily of two main components: The Ground control hardware system and the AUV control hardware system. The architecture of this system is depicted in Fig. 6.

The Ground control hardware system comprises several key components. Firstly, there is a computer that runs monitoring software responsible for reporting real-time status updates of the AUV and sending instructions to it. Secondly, an optical fiber transceiver is employed to establish a connection between the computer and the AUV controller. This optical fiber connection allows for the transmission of information

between the two systems. Lastly, a wireless communication module is attached to the computer, enabling underwater wireless communication by establishing a connection with its counterpart module in the AUV. AUV is capable to communicate through the Raspberry Pi's WiFi on the water. When underwater, it can use radio communication within a range of 4 meters depth and 150 meters away.

By integrating these components, the ground control hardware system facilitates effective communication and control of the AUV, ensuring real-time monitoring and seamless information exchange between the operator and the AUV.

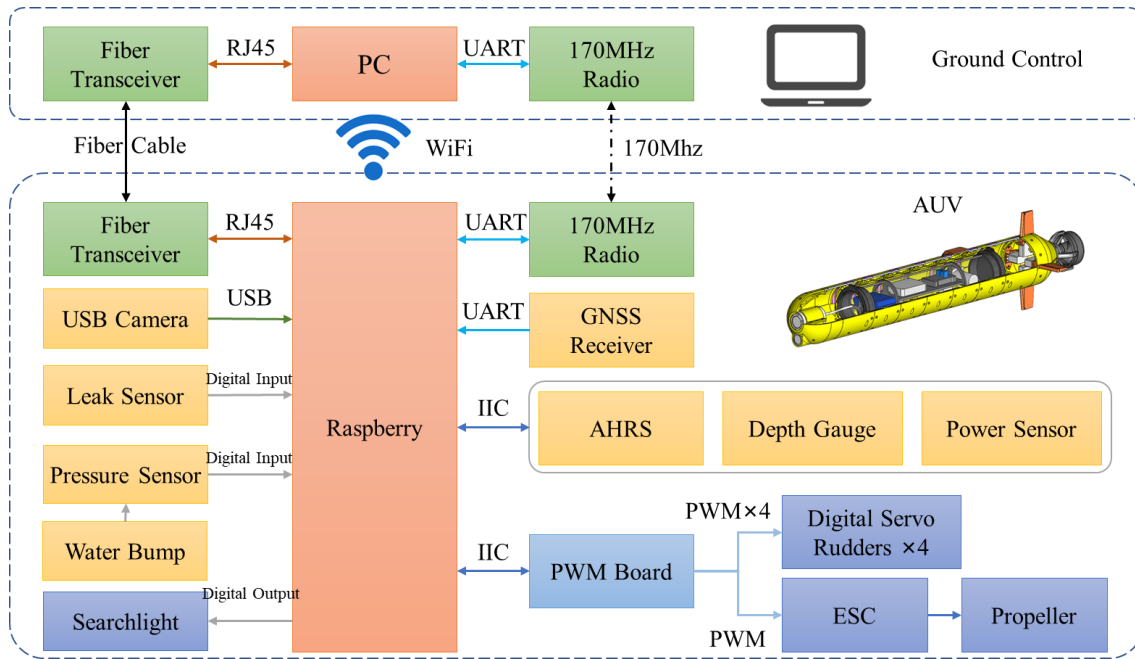


Fig. 6 Hardware system architecture

The AUV's control core is mainly responsible for the data processing and motion control and implemented using a Raspberry Pi. Additionally, the AUV utilizes various components and systems for its operations such as: attitude and heading reference system (AHRS), depth sensor, power sensor, GNSS receiver, PWM Servo Board, leak sensor, etc. [12].

The hardware system of the AUV is categorized into several subsystems based on their functions. These subsystems encompass power supply, communication, motion control, sensing, static heave, navigation and positioning, and safety protection. The power supply subsystem ensures the provision of electrical power, while the communication subsystem facilitates data exchange with the onshore control station. Motion control governs the AUV's movement, and sensing involves various sensors to gather environmental and internal data. The static heave subsystem maintains vertical stability, navigation and positioning enable accurate underwater navigation, and safety protection incorporates measures to ensure secure operation. By organizing the hardware system into these subsystems, the AUV can perform its functions effectively and safely. Detailed description of each hardware system is given as under:

1) Power supply system

The power supply system of the AUV ensures a stable power source for the entire vehicle and encompasses functions such as voltage and current monitoring, charge management, and discharge protection. It supplies different ranges of voltages to different components of the AUV, including: 5V power supply for Raspberry Pi, Attitude and Heading Reference System, and optical fiber transceiver; 12V power supply for LED lights and propeller; 3.3V power supply for the depth sensor, temperature and humidity sensor; 6.5V power supply for the steering gear. This comprehensive power supply system guarantees the reliable operation of each component by providing the appropriate voltage levels they require.

2) Communication system

The underwater vehicle has two communication modes that is wired and wireless. The wired communication is achieved through optical fiber cable, which has excellent anti-interference properties, high transmission speeds, minimal loss, and enormous communication capacities. The optical fiber is connected to the Raspberry Pi through an optical fiber transceiver inside the sealed compartment. The onshore optical fiber transceiver is connected via the optical fiber in order to implement cable communication. The wireless communication is achieved through a wireless serial port module. The module uses LoRa spread spectrum technology, which offers a long communication range and potent interference resistance. Table 2 below shows the key parameters. To establish underwater wireless connectivity, paired wireless communication modules are utilized in both the ground system and the AUV.

Table 2 Wireless communication module parameters

Operating frequency band (MHz)	Transmission power (dBm)	Communication interface	Voltage (V)
160-173.5	21-30	UART	5
Communication distance (m)	Air rate (kbps)	Size (mm)	Weight (g)
150m	0.3k-9.6k	24x43	8.2

3) Motion control system

The actuator of the system consists of the stern propeller and four steering gears. The T200 propeller, commonly used in underwater robots, is selected for its power and thrust, which meet the resistance specifications at different speeds. To fulfil the underwater steering requirements, the AUV utilizes waterproof steering gears capable of generating a powerful torque of up to 5Nm. Each of the four rudder blades can be controlled independently, enabling various experimental maneuvers such as X-rudder navigation or differential cross rudder navigation. Table 3 provides detailed specifications for the propeller and steering gears, showcasing their relevant characteristics.

Table 3 Parameters of propeller and steering gear

T200 thruster	Voltage(V)	Max power (W)	Weight (g)	Volume (mL)	Max forward thrust (N)	Speed (r/min)
	12	350	344	188	35.5	300-3800
Steering gear	Voltage(V)	Torque (N)	Weight (g)	Size (mm)	No load speed	PWM
	6.5	50	94	40x20x38.8	0.13sec/60°	1500-900 1500-2100

4) Perceptual system

The AUV is equipped with advanced sensing equipment, including a high-definition camera, LED fill light, and depth sensor, enabling efficient detection of environmental information. The specifications for the camera, LED, and depth sensor are presented in Table 4, demonstrating their respective capabilities and features. These sensing components play a crucial role in capturing clear visuals, providing illumination in dark conditions, and accurately measuring depth, enhancing the AUV's perception and understanding of its surroundings.

5) Static heave system

The water suction and drain system, serving as an additional feature of ARMs1.0, comprises a water pump, a sealed water bag, and a pressure sensor. Both the water pump and the sealed water bag are located inside the sealed cabin. The suction and drainage volume can be adjusted by modifying the pump's working time, achieving a flow rate of 225 mL/min. The water bag has a maximum capacity of 250 mL, allowing it to hold a significant amount of water. A pressure sensor is attached to the water pipe, ensuring safety during operation. As a precautionary measure, the water absorption process automatically halts once the water bag

has adequately absorbed the water and reached the upper-pressure limit. This system enables controlled water suction and drainage operations with precise monitoring and safety mechanisms in place.

Table 4 Parameters of some sensing equipment

Camera	Pixel	Voltage (V)	Weight in air (g)	Interface
	1920x1080	5	230	USB
LED	Power (W)	Voltage (V)	Weight in air (g)	Interface
	15	12	85	PWM
Depth sensor	Resolving power	Voltage (V)	Interface	
	0.2mbar	3.3	12C	

6) Navigation and positioning system

The integrated navigation system plays a vital role in providing essential navigation and positioning information for the autonomous motion control of the AUV. It consists of three main components: the attitude and heading reference system module (AHRS), the GNSS information receiver, and the depth sensor. The AHRS module is a compact chip that combines an accelerometer, gyroscope, and magnetometer, enabling accurate calculations of acceleration, attitude, heading, and other relevant data. The AUV's core controller receives positioning data from the GNSS receiver, when AUV is operating near the surface. Additionally, the depth sensor provides crucial depth information to enhance the AUV's understanding of its underwater environment. Together, these components form an integrated navigation system that enables effective and reliable autonomous control of the AUV.

7) Safety protection system

The safety protection system of the AUV encompasses various important functions to ensure the safety and integrity of the system. These functions include water leakage protection, control software heartbeat package loss protection, water absorption and drainage protection, internal temperature and humidity protection, and more. The water leakage sensor consists of a water drop collecting component, a level comparison module, and a relay. It is strategically positioned at the base of the water bag near the hatch cover to detect any water leakage. The control software heartbeat package loss protection mechanism maintains a stable connection between the ground and AUV computers, preventing the AUV from losing control. Additionally, the static heave system allows for emergency water evacuation, enabling rapid floating of the hull. To prevent overheating, a temperature sensor is installed in the cabin to monitor the temperature and send real-time data to the ground station. These safety measures collectively contribute to the reliable operation and protection of the AUV system.

2.2 Software system architecture

AUV software system design includes AUV software architecture design, onboard program writing, and onshore monitoring software development. The system architecture is shown in Fig. 7.

As depicted in Fig. 7, the AUV software operates on a Raspberry Pi platform and is programmed using C++. It establishes communication with various sensors through UART/TTL, IIC, and USB interfaces, allowing for data collection of depth, attitude, position, and other relevant parameters. This data is then fed into the motion control algorithm for calculation, resulting in basic control instructions for the thruster and servo mechanisms. Additionally, the AUV software maintains real-time connectivity with the onshore monitoring program via wireless communication, facilitating data exchange and storage in a database.

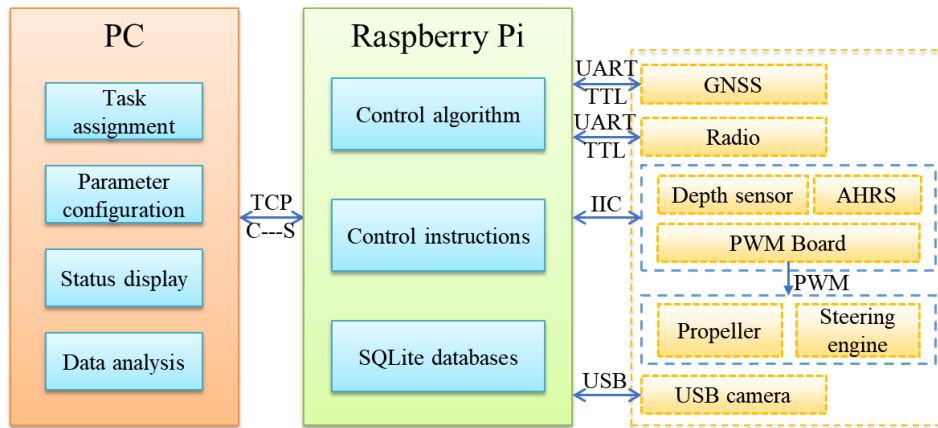


Fig. 7 Software system architecture

The ground control station software, illustrated in Fig. 8, is developed using the Qt software on a Windows 10 platform. It provides a graphical interface for real-time display of crucial AUV data such as heading, roll, pitch, voltage, rudder angle, speed, and depth. Moreover, the ground control station software offers several functionalities including task assignment, parameter configuration, safety alarm systems, as well as data storage and analysis capabilities. These features enable efficient monitoring and control of the AUV operations from the onshore station.



Fig. 8 PC monitoring software

3. Motion control algorithm

The underwater vehicle is a highly nonlinear system with coupled motions across different degrees of freedom [13]. When designing the controller, it is crucial to address the challenge of motion coupling [14]. In the case of the AUV discussed in this article, its movement during tests is relatively slow, not exceeding 2 knots, and the horizontal and vertical motions can be considered as decoupled [15-17]. However, due to the inability of AUV to obtain real-time satellite positioning underwater and the lack of high-precision navigation equipment that can calculate underwater coordinates based on pre entry coordinates, this undoubtedly poses difficulties for complex underwater maneuvers. To simplify the controller design process, the spatial motion is divided into two planes for independent investigation [18-20]. This article focuses on the algorithm design for depth tracking in the vertical plane, while the motion control in the horizontal plane is simplified to a fixed rudder angle of 0, that is, when the AUV conducts experiments such as depth tracking, it will navigate in a straight line along the initial heading angle in the horizontal plane [21]. The depth tracking control is

implemented using a hierarchical control system that combines line-of-sight (LOS) guidance, S control, and active disturbance rejection control (ADRC) technology, as illustrated in Fig. 9.

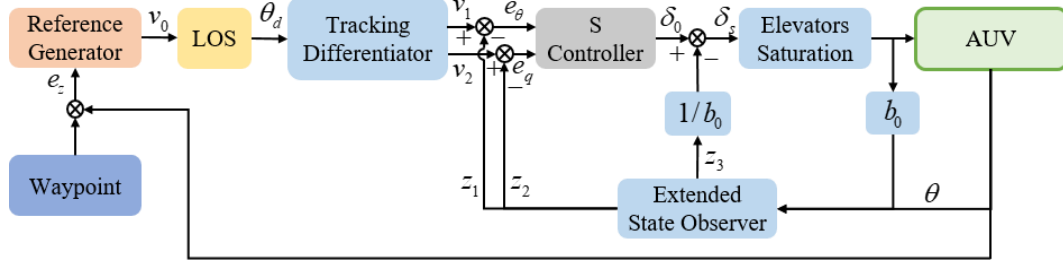


Fig. 9 Control scheme for depth tracking

The Line-of-Sight (LOS) guidance method is a well-known and commonly used strategy in guidance systems. It plays a crucial role in addressing the depth tracking problem of the AUV. By considering the desired depth, current depth, and attitude information, the LOS guidance method can provide the required pitch angle at the next time step [22]. Fig. 10 illustrates the implementation of the LOS guidance method in the context of the depth tracking problem[23].

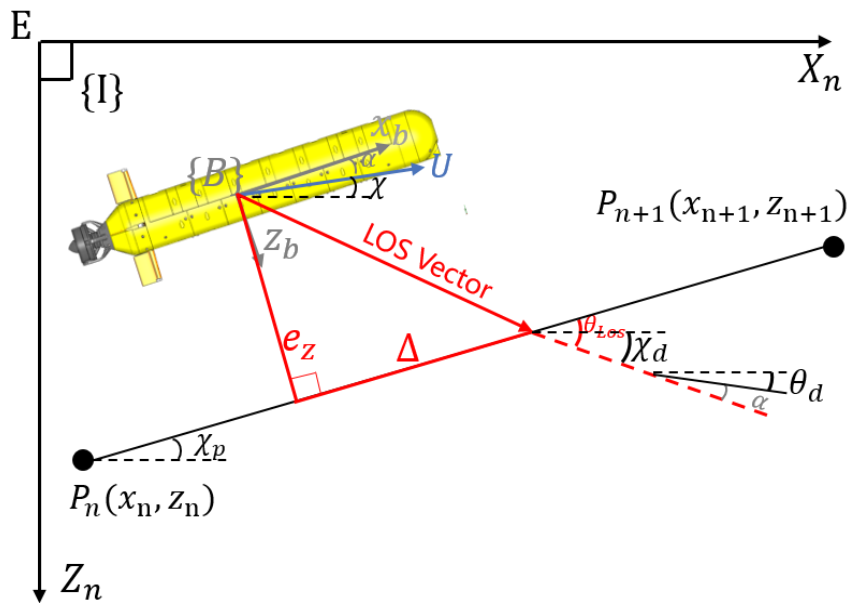


Fig. 10 LOS guidance for depth tracking

Assuming that the AUV is following the line path connecting the waypoints $P_n - P_{n+1}$ in a given depth plane as shown in Fig. 10, e_z is the cross-track error for the current position, χ_p is the vertical path-tangential angle, Δ is the projection distance of the LOS vector on the path line from the current position of the AUV to the sight point. The orientation of the LOS vector determines the desired elevation angle χ_d , which can be mathematically expressed as follows:

$$\chi_d = \theta_{LOS} + \chi_p = \tan^{-1}(e_z / \Delta) + \chi_p \quad (1)$$

When conducting a fixed depth tracking task, waypoints P and $P+1$ are at the same depth, and at this point χ_p is 0, the desired elevation angle $\chi_d = \theta_{LOS}$. The desired elevation angle of the AUV can be expressed as the sum of the desired pitch θ_d and the angle of attack α . However, in most cases, the influence of the attack angle can be ignored for underwater vehicles. Therefore, the desired pitch angle of the AUV can be calculated using the LOS strategy and input into the control algorithm to obtain the control instruction for the rudder angle. This allows for effective control of the AUV's motion in the desired depth plane.

S control and Active disturbance rejection control (ADRC) are the foundations on which the controller for ARMs1.0 was created. Among these, the S controller combines PID control and fuzzy control to create a straightforward and reliable nonlinear controller. This fusion of control techniques allows for effective handling of nonlinearity and uncertainty in the system, resulting in improved control performance and stability [24]. ADRC is an advanced control technology that inherits the core idea of PID and does not rely on the precise model of the controlled object. Its unique feature is that all uncertain factors acting on the controlled object are summarized as "composite disturbances", and unknown composite disturbances are estimated and compensated using the input and output data of the controlled object.

The S control algorithm is shown as,

$$\begin{cases} u_i = 2.0 / (1.0 + \exp(-k_{i1}e_i - k_{i2}\dot{e}_i)) - 1.0 + \Delta u_i \\ f_i = K_i u_i \end{cases} \quad (2)$$

where, e_i and \dot{e}_i are the control inputs corresponding to freedom i , u_i is the control output of freedom i , k_{i1} and k_{i2} is respectively the control parameter corresponding to deviation and deviation change rate in freedom i , f_i is the force desired of the corresponding freedom and K_i is the maximum force or moment that the actuator can supply in this freedom. Δu_i is fixed disturbing force (normalization) got through adaptive method.

It is clear from the equations that the S control and PD control are extremely similar. The former is nonlinear in comparison to the latter, thus fitting a nonlinear system is preferable than using a linear function. However, the S control lacks a local adjustment function and adaptive adjustment simply approximates the system, making Δu_i inaccurate and unable to obtain the optimal fit due to the complexity and unpredictability of the control object [25].

The extended state observer (ESO) is the core element of ADRC. It treats internal uncertainty and external disturbances as a total disturbance, transforming control problems into the estimation and suppression of total disturbances. This approach enables real-time estimation and compensation, simplifying the control problems significantly. ADRC incorporates components such as the tracking differentiator, nonlinear feedback combination, and total disturbance estimation and rejection [26, 27]. The ADRC architecture is depicted in Fig. 9, and the corresponding control algorithm is represented by equation (3) as follows:

$$\begin{cases} fv = fhan(v_1 - v, v_2, r_0, h) \\ v_1 = v_1 + hv_2 \\ v_2 = v_2 + hfv \\ e = z_1 - y \\ fe = fal(e, 0.5, \delta), \quad fe_1 = fal(e, 0.25, \delta) \\ z_1 = z_1 + hz_2 - \beta_{01}e \\ z_2 = z_2 + h(z_3 + b_0u) - \beta_{02}fe \\ z_3 = z_3 - \beta_{03}fe_1 \\ e_1 = v_1 - z_1 \quad e_2 = v_2 - z_2 \\ u = -\frac{fhan(e_1, ce_2, r, h_1) + z_3}{b_0} \end{cases} \quad (3)$$

where v_1 is the desired trajectory and v_2 is its derivative, r is the amplification coefficient that corresponds to the limit of acceleration, c is a damping coefficient to be adjusted in the neighbourhood of unity, h_1 is the precision coefficient that determines the aggressiveness of the control loop and it is usually a multiple of the

sampling period h by a factor of at least four, and b_0 is a rough approximation of the coefficient b in the plant within a $\pm 50\%$ range, β_{01} , β_{02} , β_{03} are the observer gains of ESO.

The choice of the control law (u) in equation (3) can vary depending on the specific requirements and characteristics of the system. Different control laws can be selected based on the desired control objectives and performance criteria. In this article, the nonlinear feedback combination is selected as S control. At the same time, based on the real-time estimation and compensation of total disturbance through ESO by ADRC, the disadvantage of inaccurate Δu_i estimation in S control is compensated. Therefore, the output of the control can be expressed as

$$u_i = 2.0 / (1.0 + \exp(-k_{i1}e_i - k_{i2}\dot{e}_i)) - 1.0 - z_3/b_0 \quad (4)$$

4. Experiment results

The AUV performed the underwater tests in towing tank facility of Huazhong University of Science and Technology as well as in the open waters at 'Yujia Lake' in Wuhan City China. The objective of these tests was to assess the maneuverability of the AUV in both the vertical and horizontal planes, gather actual test data for CFD simulation, and further enhance the structural design of the AUV's mechanical system. To evaluate the AUV's maneuverability, a zigzag maneuverability test and a turning test were conducted. Additionally, a depth tracking test was performed to assess the AUV's path tracking capability and enhance its underwater path planning and guidance abilities.

4.1 Zigzag maneuverability test in depth plane

The primary purpose of the vertical Zigzag test was to evaluate the maneuverability of the AUV in the vertical plane. The test involved maintaining a steady depth and observing the change in depth with change in horizontal rudder angle and pitch angle adjustments. The AUV was initially set at a specific depth and sailed steadily. Then, the horizontal rudder angle was changed to a predetermined value, and the pitch angle was gradually adjusted until it reached the desired value. This process was repeated multiple times to replicate the test conditions and collect data for analysis and evaluation.

As depicted in Fig. 11, the depth curve is shown on the left, and the pitch curve is displayed on the right. Initially, the AUV has achieved 2m depth in 30 seconds while started at depth of 0.5 m as shown in Fig. 11. However, the AUV's forward speed was set to 1 m/s and was maintained while operating at a depth of 2 m. The AUV sailed steadily and successfully reached the desired depth within a duration of 60s. Subsequently, the AUV conducted the zigzag test. Once the desired pitch angle was adjusted to 20° , with the horizontal rudder angle set and maintained at 20° , the AUV gradually began to ascend. As the pitch angle reached 20° , the horizontal rudders were lowered, resulting in a pitch angle of -20° . Following three steering cycles, the task was completed, and the AUV floated to the surface.

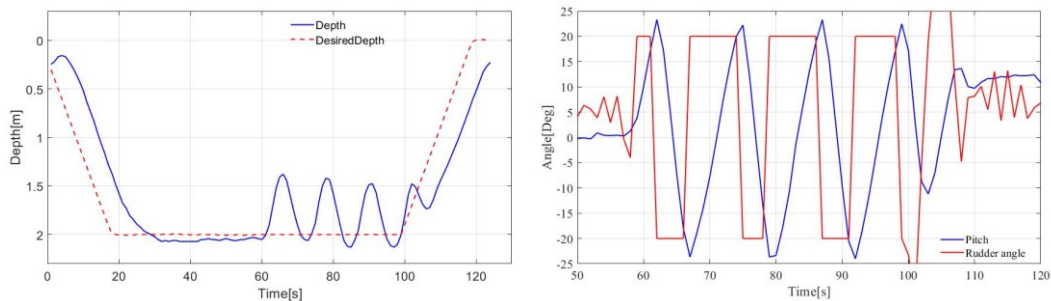


Fig. 11 Depth and pitch curve

4.2 Turning test in horizontal plane

To evaluate the maneuverability of the AUV in the horizontal plane and validate it against CFD simulation, water surface turning tests were conducted. Initially, the AUV navigated along a straight line at a

constant speed. After a certain duration, set the rudder angle to 10° and initiated the turning process. The test concluded once the heading rotation was complete. The GPS positioning data was automatically recorded by the computer to generate a curve and calculate the turning radius based on the speed and rudder angle. CFD simulation and test results are shown in the Table 5 and Fig. 12, where δ is the rudder Angle, the speed u before turning is about 1m/s , the simulation diameter D_S is about 9.5m , and the test diameter D_T is about 9.9m .

Table 5 Turning test result

Maneuver type	Parameters	Simulation	Test	Absolute error	Relative error
$\delta=10^\circ$, $u \approx 1.0\text{m/s}$	Circle diameter	$D_S = 9.5\text{m}$	$D_T = 9.9\text{m}$	0.4m	4.04%

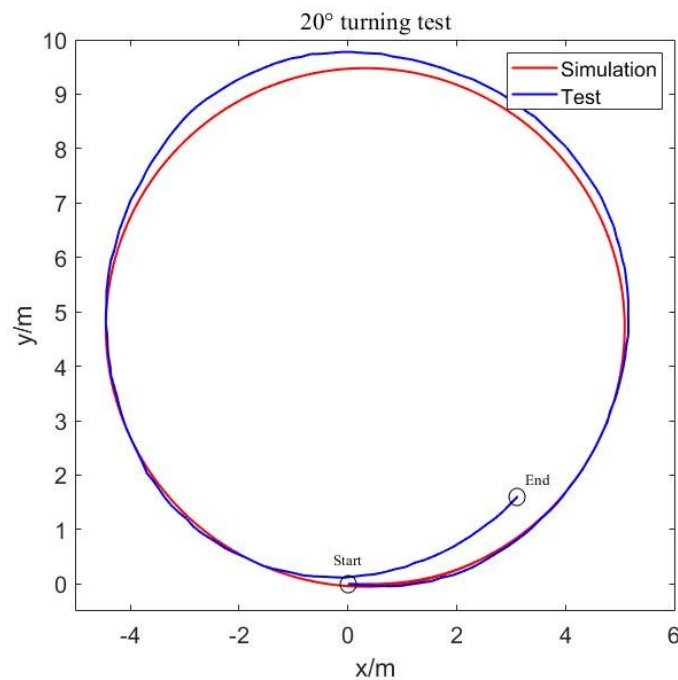


Fig. 12 Comparison results of turning test

4.3 Depth tracking test

To assess the AUV's capability for path tracking in the depth plane, an underwater depth-tracking test was conducted. As depicted in Fig. 13, the first figure illustrates the test scene for AUV maneuvering at a depth of 2m during fixed depth motion. The subsequent figures depict the depth change curve, and the pitch change curve. In this test, the AUV was set to navigate at a depth of 2m for a duration of 100s , while maintaining a speed of approximately 1m/s . Upon receiving the command, the AUV initiated its steering and diving maneuvers. It successfully reached the desired depth in approximately 25s and continued to sail along the 2m depth surface. After sailing for 80s , the mission concluded, and the AUV autonomously surfaced for data transmission. The test results demonstrate that the AUV exhibits excellent tracking ability in the depth plane, with an average depth error of less than 0.1m during stable navigation at a depth of 2m .

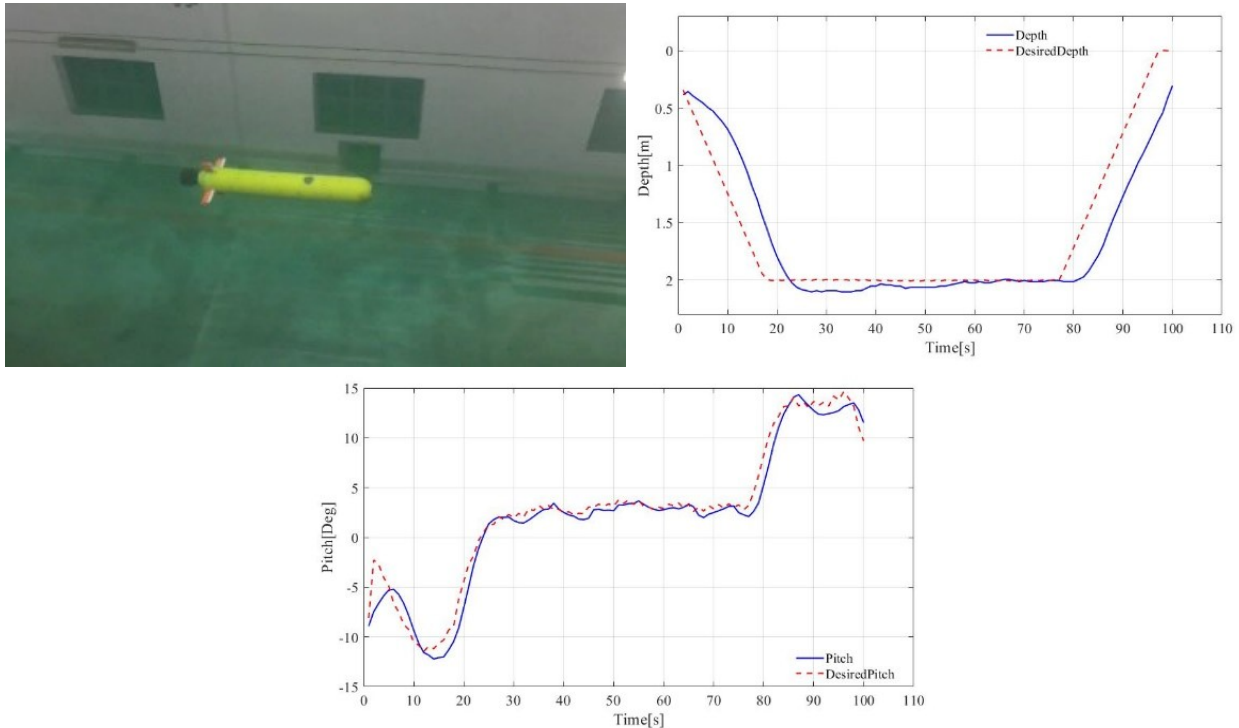


Fig. 13 Test site and depth tracking result

5. Conclusions

The design and development of the modular small AUV, named as ARMs1.0, based on 3D printing technology, have been comprehensively described. The modular design approach offers several advantages, which have been discussed in detail. By adopting a modular design, the AUV exhibits enhanced function expansion capabilities and maintainability. It also possesses the benefits of being cost-effective, highly reliable, and easily adaptable for further development.

To assess the physical maneuvering performance of the AUV, extensive underwater motion tests were conducted in both horizontal and vertical planes. These tests were carried out in a towing tank and an open water lake environment. The AUV successfully executed various desired maneuvering missions, including circle patterns, pitching, yawing, and depth tracking. These maneuvers demonstrated the AUV's capability to perform the research tasks efficiently and at a low cost.

Overall, the experimental test results revealed that the developed AUV exhibited excellent working performance with respect to horizontal and vertical plane dynamics, and depth tracking control. Thus, the AUV's design and ability to accomplish the desired maneuvering missions highlighted its suitability for a wide range of research applications.

6. Acknowledgement

This work is supported in part by the Hubei Provincial Natural Science Foundation for Innovation Groups (under Grant 2021CFA026), in part by National Natural Science Foundation of China (under Grant 52071153 and 52131101).

REFERENCES

- [1] Jian, G., Pu-Guo, W., Wei-Sheng, Y., Fu-Bin, Z., 2017. Development and trails of the distributed control system for a portable autonomous underwater vehicle. *Control Engineering of China*, 24(02), 315-320.
- [2] Hou, S., Zhang, Z., Lian, Xing, X., Gong, H., Xu, X., 2022. Hull shape optimization of small underwater vehicle based on kriging-based response surface method and multi-objective optimization algorithm. *Brodogradnja*, 73(3), 111-134. <https://doi.org/10.21278/brod73307>

- [3] Ljulj, A., Slapničar, V., Brigić, J. 2022. Unmanned surface vehicle-Triton. *Brodogradnja*, 73(3), 135-150. <https://doi.org/10.21278/brod73308>
- [4] Xu, H., Zhang, G. C., Sun, Y. S., Pang, S., Wang, X. B., 2019. Design and experiment of a plateau data-gathering AUV. *Journal of Marine Science and Engineering*, 7(10), 376. <https://doi.org/10.3390/jmse7100376>
- [5] Liu, C., Xiang, X. B., Huang, J. Yang, S. L., Zhang, S. Z., Su, X., Zhang, Y. F., 2022. Development of USV autonomy: architecture, implementation and sea trials. *Brodogradnja*, 73(1), 89-107. <https://doi.org/10.21278/brod73105>
- [6] Faheem A., Xiang, X. B., Jiang, C. C., Xiang, G., Yang, S. L., 2023. Survey on traditional and AI based estimation techniques for hydrodynamic coefficients of autonomous underwater vehicle. *Ocean Engineering*, 268, 113300. <https://doi.org/10.1016/j.oceaneng.2022.113300>
- [7] Zhou, G. Z., Xiang, X. B., Liu, C., 2023. Parameter identification and model prediction path following control of underactuated AUV: Methodology and experimental verification. *Control Engineering Practice*, 141, 105729. <https://doi.org/10.1016/j.conengprac.2023.105729>
- [8] Lakshmi, M. M., Stefano B., 2023. Effect of amplitudes and frequencies on Virtual Planar Motion Mechanism of AUVs, Part I: Forces, moments and hydrodynamic derivatives. *Ocean Engineering*, 286, 115512. <https://doi.org/10.1016/j.oceaneng.2023.115512>
- [9] Furlong, M. E., Paxton, D., Stevenson, P., Pebody, M., Perrett, J. 2012. Autosub Long Range: A long range deep diving AUV for ocean monitoring. *2012 IEEE/OES Autonomous Underwater Vehicles (AUV)*, IEEE, 2012, 1-7. <https://doi.org/10.1109/AUV.2012.6380737>
- [10] Stokey, R. P., 2005. Development of the REMUS 600 autonomous underwater vehicle. *OCEANS Proceedings of MTS/IEEE*. 2, 1301-1304.
- [11] Philips, A. B., Steenson, L. V., Rogers, E., Turnock, S. R., Harris, C. A., Furlong, M., 2013. Delphin2: an over actuated autonomous underwater vehicle for manoeuvring research. *Transactions of The Royal Institution of Naval Architects Part A: International Journal of Maritime Engineering*, 155 (A4), 171-180. <https://doi.org/10.5750/ijme.v155iA4.907>
- [12] Zhang, Q., Zhang, J. L., Ahmed C., Xiang, X. B., 2018. Virtual Submerged Floating Operational System for Robotic Manipulation. *Complexity*, 2018, 1-18. <https://doi.org/10.1155/2018/9528313>
- [13] Lapierre L, Jouvencel, B., 2007. Nonlinear Path Following Control of an AUV. *Ocean Engineering*, 34(2), 1734-1744. <https://doi.org/10.1016/j.oceaneng.2006.10.019>
- [14] Zhang, J. L., Xiang, X. B., Li, W. J., Zhang, Q., 2023. Adaptive Neural Control of Flight-Style AUV for Subsea Cable Tracking under Electromagnetic Localization Guidance, *IEEE/ASME Transactions on Mechatronics*, 28(5), 2976-2987. <https://doi.org/10.1109/TMECH.2023.3256707>
- [15] Wang, X. W., Yao, X. L., Xia, Z. P., Jiang, X. G., 2020. 3D Straight-line Path-following Control for Underactuated AUV. *Control Engineering of China*, 27(06), 977-983.
- [16] Wang, B., Su, Y. M., Qin, Z. B., 2009. Research on maneuverability and simulation of small autonomous underwater vehicle. *Journal of System Simulation*, 21(13), 4149-4148.
- [17] Wang, Z. G., Wei, Z. Y., Yu, C. Y., Cao, J. J., Yao, B. H., Lian, L., 2023. Dynamic modeling and optimal control of a positive buoyancy diving autonomous vehicle. *Brodogradnja*, 74(1), 19-40. <https://doi.org/10.21278/brod74102>
- [18] Do, K. D., Pan, J., 2004. State-and output-feedback robust path-following controllers for underactuated ships using serret-frenet frame. *Ocean Engineering*, 31(5/6), 587-613. <https://doi.org/10.1016/j.oceaneng.2003.08.006>
- [19] Pan, X., Feng, G. L., Hou, X. G., 2021. Research on AUV path tracking technology based on hierarchical reinforcement learning. *Journal of Naval University of Engineering*, 33(03), 106-112.
- [20] Li, Z. Y., Liu, W. D., Li, L., Zhang, W. B., Guo, L. W., 2021. Path following method for AUV based on Q-Learning and RBF neural network. *Journal of Northwestern Polytechnical University*, 39(03), 477-483. <https://doi.org/10.1051/jnwpu/20213930477>
- [21] Liu, C., Xiang, X. B., Duan, Y., Yang, L. C., Yang, S. L., 2024. Improved path following for autonomous marine vehicles with low-cost heading/course sensors: comparative experiments. *Control Engineering Practice*, 142, 105740. <https://doi.org/10.1016/j.conengprac.2023.105740>
- [22] Lekkas, A. M., Fossen, T. I., 2014. Integral los path following for curved paths based on a monotone cubic hermite spline parametrization. *IEEE Transactions on Control Systems Technology*, 22(6), 2287-2301. <https://doi.org/10.1109/TCST.2014.2306774>
- [23] Li, J. J., Xiang, X. B., Yang, S. L., 2022. Robust adaptive neural network control for dynamic positioning of marine vessels with prescribed performance under model uncertainties and input saturation. *Neurocomputing*, 484, 1-12. <https://doi.org/10.1016/j.neucom.2021.03.136>
- [24] Bo, W., Yu, M. S., Lei, W., Yue, M. L., 2009. Modeling and motion control system research of a mini underwater vehicle. *2009 International Conference on Mechatronics and Automation*, 9-12 August, Changchun, China, 4463-4467.
- [25] Liu, X. M., Xu, Y. R., 2001. S control of automatic underwater vehicles. *The Ocean Engineering*, 19(3), 81-84.

- [26] Han, J., 2009. From PID to active disturbance rejection control. *IEEE Transactions on Industrial Electronics*, 56(3), 900-906. <https://doi.org/10.1109/TIE.2008.2011621>
- [27] Li, J. J., Xiang, X. B., Dong, D. L., Yang, S. L., 2023. Prescribed time observer based trajectory tracking control of autonomous underwater vehicle with tracking error constraints. *Ocean Engineering*, 274, 114018. <https://doi.org/10.1016/j.oceaneng.2023.114018>